Published in final edited form as:
Exp Eye Res. 2010 September ; 91(3): 336–346. doi:10.1016/j.exer.2010.05.019.

Solvent accessibility of βB2-crystallin and local structural changes due to deamidation at the dimer interface

Takumi Takata[a,*], **Joshua P. Smith**[a,*], **Brian Arbogast**[b], **Larry L. David**[c], and **Kirsten J. Lampi**[a]

[a] Oregon Health and Science University, Integrative Biosciences, 611 SW Campus Dr., Portland, OR 97239

[b] Oregon State University, Environmental Health Sciences, Corvallis, Oregon 97331

[c] Oregon Health and Science University, Biochemistry and Molecular Biology, Sam Jackson Rd., Portland, OR 97239

Abstract

In the lens of the eye the ordered arrangement of the major proteins, the crystallins, contributes to lens transparency. Members of the β/γ-crystallin family share common β-sheet rich domains and hydrophobic regions at the monomer-monomer or domain-domain interfaces. Disruption of these interfaces, due to post-translational modifications, such as deamidation, decreases the stability of the crystallins. Previous experiments have failed to define the structural changes associated with this decreased stability.

Using hydrogen/deuterium exchange with mass spectrometry (HDMS), deamidation-induced local structural changes in βB2-crystallin were identified. Deamidation was mimicked by replacing glutamines with glutamic acids at homologous residues 70 and 162 in the monomer-monomer interface of the βB2-crystallin dimer. The exchange-in of deuterium was determined from 15 sec to 24 h and the global and local changes in solvent accessibility were measured.

In the wild type βB2-crystallin (WT), only about 20% of the backbone amide hydrogen was exchanged, suggesting an overall low accessibility of βB2-crystallin in solution. This is consistent with a tightly packed domain structure observed in the crystal structure. Deuterium levels were initially greater in N-terminal domain (N-td) peptides than in homologous peptides in the C-terminal domain (C-td). The more rapid incorporation suggests a greater solvent accessibility of the N-td.

In the βB2-crystallin crystal structure, interface Gln are oriented towards their opposite domain. When deamidation was mimicked at Gln70 in the N-td, deuterium levels increased at the interface peptide in the C-td. A similar effect in the N-td was not observed when deamidation was mimicked at the homologous residue, Gln162, in the C-td. This difference in the mutants can be explained by deamidation at Gln70 disrupting the more compact C-td and increasing the solvent accessibility in the C-td interface peptides.

When deamidation was mimicked at both interface Gln, deuterium incorporation increased in the C-td, similar to deamidation at Gln70 alone. In addition, deuterium incorporation was decreased in

Corresponding Author: lampik@ohsu.edu.
*These authors contributed equally to the paper.

the N-td in an outside loop peptide adjacent to the mutation site. This decreased accessibility may be due to newly exposed charge groups facilitating ionic interactions or to peptides becoming more buried when other regions became more exposed.

The highly sensitive HDMS methods used here detected local structural changes in solution that had not been previously identified and provide a mechanism for the associated decrease in stability due to deamidation. Changes in accessibility due to deamidation at the interface led to structural perturbations elsewhere in the protein. The cumulative effects of multiple deamidation sites perturbing the structure both locally and distant from the site of deamidation may contribute to aggregation and precipitation during aging and cataractogenesis in the lens.

Keywords

lens; β-crystallins; deamidation; hydrogen/deuterium exchange with mass spectrometry; 3D structure

1. Introduction

Cataract formation is a major cause of blindness worldwide (Resnikoff et al., 2004). Age related cataracts are associated with an accumulation of aggregated and precipitated lens protein (Harding, 1969; Truscott and Augusteyn, 1977). To maintain clarity, lens structural crystallins are packed as higher order oligomers and form complex crystallin-crystallin interactions (Delaye and Tardieu, 1983). The lens has little turnover. Therefore, post-translationally modified crystallins remain during one's lifetime and the stabilizing interactions are disrupted. Comprehensive proteomics has identified deamidation as the most prevalent modification in the insoluble proteins in aged and cataractous lenses (Hains and Truscott, 2007; Hanson et al., 2000; Wilmarth et al., 2006).

Deamidation has been identified at several highly conserved glutamine/asparagine residues at key interacting interfaces in β/γ-crystallins (Searle et al., 2005; Wilmarth et al., 2006; Zhang et al., 2003). Crystal structures of β-crystallin subunits have revealed two highly homologous and β-sheet rich domains that are connected by a linker peptide (Bax et al., 1990; Nalini et al., 1994; Van Montfort et al., 2003). The β-crystallin dimers contain an interface between the domains or between the monomer subunits. This interface is stabilized by hydrophobic interactions and hydrogen bonding (Lapatto et al., 1991; Liu et al., 2006).

We have reported that deamidation at the interface in βB1-, βB2- and βA3-crystallins decreased their stabilities and altered subunit-subunit interaction *in vitro* (Lampi et al., 2001, 2006; Takata et al., 2007, 2009). In the βB1-crystallin, deamidation at the interface increased oligomerization (Lampi et al., 2001). The deamidation mimic at the conserved glutamines in the domain-domain interface of monomeric γD-crystallin similarly decreased stability (Flaugh et al., 2006). Even though deamidation at these hydrophobic interfaces significantly decreased protein stability, only subtle changes were detected in the structure and no dissociation of the dimer occurred.

In this study, we used hydrogen/deuterium exchange with mass spectrometry (HDMS) to investigate local effects of deamidation on the βB2 monomer-monomer interface. This is the first report detecting deuterium incorporation in lens β-crystallins with mass spectrometry, and it elucidates the effect of deamidation on crystallin structure at the peptide level. We have demonstrated that 1) there are differences in solution dynamics between the highly homologous domains of βB2, and that the 2) homologous domains were perturbed differently by interface deamidations.

2. Methods and materials

2.1. Materials and Sample Preparation for Hydrogen/Deuterium Exchange

Deuterium oxide (99.9 atom %D) was purchased from Sigma (St. Louis, MO). Immobilized pepsin and TCEP were obtained from Pierce (Rockford, IL). Digestion tubes for peptic digestion were purchased from Millipore (Bedford, MA). All other chemicals were purchased from Fisher Scientific (Pittsburg, PA).

Wild type (WT), Q70E, Q162E, and double mutant Q70E/Q162E (DM) βB2 were recombinantly expressed in *E. coli* as previously reported (Lampi et al., 2006). WT βB2 was purified by successive ion-exchange chromatography as reported previously (Lampi et al., 2006) with an additional chromatography step using a SP Sepharose cation exchange column (Amersham Bioscience, Pisscataway, NJ) equilibrated in a 50 mM MES buffer (pH 6.1), 0.6 mM EDTA and 1 mM DTT. The DM βB2 was first applied to a SP Sepharose cation exchange column equilibrated in the same MES buffer followed by a second chromatography step on a DEAE Fast Flow anion exchange column (Amersham) equilibrated in a 20 mM Tris buffer (pH 7.4) containing 0.6 mM EGTA, 1 mM EDTA, and 1 mM DTT. The purity and mutation sites mimicking deamidation were checked by SDS-PAGE and mass spectrometry (LTQ, ThermoFinnigan, San Jose, CA) with trypsin digestion.

Proteins were concentrated to 10.0 mg/ml and dialyzed into 100 mM sodium-phosphate (pH 7.0), 2.5 mM TCEP, and 2 mM EDTA in H_2O (Buffer A). All proteins were flash frozen in liquid nitrogen and kept in −80 °C until used. Concentrations were calculated from UV absorbance at 280 nm with extinction coefficients for βB2 of 1.7 $(mg/mL)^{-1}cm^{-1}$.

2.2. Bis-ANS Fluorescence assay

The hydrophobicity of βB2 was determined by bis-ANS fluorescence. Each of the 1 μM protein samples was vortexed on ice for 2 min or vortexed at ambient temperature for 4 min and was mixed with bis-ANS stock solution in Buffer A. The 20 μl of bis-ANS stock solution (5.0×10^{-4} M of bis-ANS) was added to 3 ml of sample solution (1.0×10^{-8} M). After 15 min of incubation at ambient temperature bis-ANS fluorescence was measured on a Photon Technology International QM-2000-7 spectrometer using the manufacture's supplied software, FeliX (Photon Technology International, Lawrenceville, NJ). Slit widths were set to 2 nm. Bis-ANS fluorescence emissions were scanned between 420 and 550 nm with an excitation wavelength of 395 nm.

2.3. Global Hydrogen/Deuterium Exchange

Methods for both global and local hydrogen/deuterium exchange with mass spectrometry followed previously published methods by Dr. Max Deinzer (Yan, et al., 2004; Yan and Maier, 2009; Yan, et al., 2002).

HDMS for the native protein was initiated by diluting 15 μL of the protein solution 10-fold with 135 μL of Buffer A only made with D_2O (pD 7.0, Buffer B). Protein solution exchanged in D_2O was incubated at 25 °C for various time (15 sec, 1 min, 4 min, 15 min, 60 min, 24 hours). At each time 25 μL of deuterated protein solution was aliquoted into a pre-chilled tube containing quenching buffer (25μL of 0.42 % phosphoric acid made with H_2O). Under these quenching conditions the pH/pD of all solution was kept at 2.6 to decrease back exchange (Englander et al., 1996). Samples were flash frozen with liquid nitrogen until analysis by mass spectrometry within 24 hours. For the global hydrogen exchange, samples were directly loaded onto the HPLC. During chromatography the buffers, connecting tubes and the trap column were submerged in an ice-bath to minimize deuterium back-exchange (Zhang et al., 1993). The protein samples were desalted on a trap column (0.18 mm x 20

mm, Waters Atlantis C18) for one minute at 15ul/min, then eluted to a packed spray tip (100um × 5 cm of Hamilton PRP-3) with a fast gradient of 15–90% Buffer B at 1ul/min. The mass spectrometer was a Waters Q-TOF Ultima Global (Waters, Milford, MA) with a nano-ESI ion source. (Waters). The samples were injected and the gradients run with a Waters NanoAcquity UPLC. Proteins eluted in 6–7 minutes. The eluants were 0.1% formic acid in water (pump A) and in acetonitrile (pump B). The multiple charge states were deconvoluted using MaxEnt 1 software (Waters).

Deuterium levels in mutant proteins were compared to WT samples that were analyzed under the same chromatography conditions and on the same day. Proteins were never fully deuterated, even in the presence of a denaturant, because of the compact structure of the β-crystallins and the tendency to precipitate upon unfolding. Therefore, back-exchange from a totally deuterated sample was not able to be determined and instead relative levels of deuterium were reported. Results are the average of two or three independent experiments where noted.

2.4. Local Hydrogen/Deuterium Exchange

Hydrogen exchange was performed as described above and the quenched samples were flash frozen with liquid nitrogen until ready for proteolysis with pepsin. Pepsin digestion was performed in a pre-washed Millipore centrifugal filter tube containing immobilized pepsin. The bottom of the tube was covered with parafilm, placed in an ice bath (25 μL of sample: 30 μL of pepsin slurry), and vortexed for 2 min. The digestion was stopped by centrifugation (3000 g x 5 sec) in order to separate the immobilized pepsin beads from the protein solution. The protein solution was collected in a pre-chilled tube and flash frozen in liquid nitrogen until analysis. Following digestion, samples were stored at −80 °C until analysis by mass spectrometry. Nondeuterated proteins were also digested in order to determine all possible peptic peptides and act as a non-deuterated control.

The level of deuterium incorporation into peptide fragments was determined by Q-TOF Ultima Global in-line with RP-UPLC (Waters NanoAcquity). During chromatography buffers, connecting tubes, trap and analytical columns were submerged in an ice-bath and the auto sampler was cooled to minimize back exchange of deuterium. The mixtures of peptides were desalted on a trap column (0.18 mm × 20 mm Waters Atlantis) for one minute with 3% acetonitrile in 0.1% formic acid, then applied to the separating C18 column (0.1 mm × 100 mm, Waters BEH C18) at a flow rate of 0.47 ul/min and separated during a 14 min gradient of 25 to 85% acetonitrile/H_2O. Both mobile phases contained 0.1% formic acid. Eluted peptides were loaded into the Q-TOF Ultima Global (Waters) with a nano-ESI ion source, and peak distribution was analyzed by Mass Lynx software (Waters). Separate samples were prepared and analyzed for the 4 min time point of WT and DM, and standard error was reported.

In a separate set of experiments the level of deuterium incorporation into peptide fragments was determined by LTQ-Orbitrap Discovery (15000 resolution) with Accela Autosampler (Thermo Scientific, USA). During chromatography trap and analytical columns were submerged in an ice-bath to minimize back exchange of deuterium, and the auto sampler was at 2 °C. The mixtures of peptides were desalted on the trap column for two minutes with 2% acetonitrile in 0.1% formic acid at 0.200 ml/min, then applied to the separating C18 column (50 mm × 2.1 mm, Bio Basic C18) at a flow rate of 0.300 ml/min and separated during an 8 min gradient of 10 to 80% acetonitrile/H_2O. Both mobile phases contained 0.1% formic acid. Eluted peptides were loaded into the LTQ-Orbitrap Discovery (Thermo Scientific), and isotopic peak distributions were analyzed by HD Desktop (Pascal et al., 2009). Independent experiments were repeated for two to three times for WT and DM, and standard error was reported.

In order to determine the rate of back exchange, several β-crystallins were deuterated by repeated freeze-drying in D_2O buffers or by denaturation in D_2O buffer containing Gdn-HCl. Under either of these conditions, a low recovery of soluble protein and deuterium incorporation levels around 50–70% prevented analysis of 100% deuterated peptide controls. Instead, samples were handled identically in order to compare WT and mutant peptides directly.

2.5. Data Analysis for deuterated peptides

Data acquisition and additional spectral analysis for HDMS were performed using Mass Lynx software (Waters). Peptide assignments were made using Mascot (Perkins et al., 1999) at matrixscience.com (http://www.matrixscience.com/home.html). Deuterated peptides were identified based on parent masses from the peptic peptide map. The isotopic spectral centroid data of each ion mass were acquired and calculated using HX-Express software (Weis et al., 2006) at HXMS.com (http://www.hxms.com/hxms.htm). Data were plotted versus time. The relative deuterium level was calculated by the following equation (1)

$$d = m - m_{0\%} \tag{1}$$

and the relative percent deuterium by (2)

$$d_{\%} = \left(\frac{m - m_{0\%}}{m_{100\%} - m_{0\%}} \right) \times 100, \tag{2}$$

where d is the relative deuterium level in a peptic peptide, $d_{\%}$ is the relative percent deuterium, m is the centroid molecular weight of an observed partially deuterated peptide, $m_{0\%}$ is the centroid molecular weight from the undeuterated peptide, and $m_{100\%}$ is the centriod molecular weight from the 24 hour deuterated peptide, respectively.

2.6. Electrophoresis

Electrophoresis was performed using precast, 1.0 mm thick 8 × 8 cm, polyacrylamide NuPAGE 10% Bis-Tris gels (Invitrogen, Carlsbad, CA). Proteins were visualized by staining with SimplyBlue SafeStain (Invitrogen).

3. Results

3.1. Global Conformational Changes due to deamidation in βB2

The overall conformation and solvent accessibility was determined by global HDMS. The whole mass of the WT βB2 monomer increased from 23,250 to 23,286 after 24 hours of incubation in D_2O buffer. In the βB2 monomer there are 192 amide hydrogen available for exchange with deuterium. The 36 Da increase in mass reflected a 19% incorporation of deuterium. The relative deuterium levels in individual peptic peptides were summed and totaled 39 Da, in close agreement with the global exchange analysis. The deuterium incorporation of 24–25 Da was similar between all proteins at 15 sec and similar between WT and the single mutants, Q70E and Q162E, at 24 h, increasing to 36–39 Da. Experiments were repeated for WT and an average of 40±12 Da (N=3) were incorporated after 24 h. There was a trend towards increased deuterium level in the double mutant, Q70E/Q162E (DM), compared to WT at 60 min and at 24 h in 2 independent experiments. However, the increase was within the variability of the data. This low deuterium incorporation for all

proteins is indicative of the tightly packed β-sheet content of the Greek-key motif structure observed in the X-ray crystal structure.

Bis-ANS fluorescence intensity was also greater for the DM than for WT (Fig. 1), indicating greater hydrophobicity, which would result from an increased exposure of previously buried regions.

These data are in agreement with our previous analyses of the overall 3D structure of βB2-crystallin (Lampi et al., 2006), which showed only subtle changes in the overall 3-D structure due to deamidation.

3.2. Peptic peptide mapping and mass spectra of βB2-crystallin

Nondeuterated βB2-crystallin was digested with pepsin, and the resulting peptic peptides were identified by their parent ion masses and ms/ms spectra with Sequest search. These masses were then used to identify peptic fragments from the deuterated samples that were analyzed during a much shorter chromatography time to prevent back-exchange. Between 17 and 23 peptic peptides were recovered for each protein and ranged in length from 8 to 23 amino acids. Peptic peptides were recovered from the entire sequence of WT and the DM (residues 1–204) and nearly the entire sequence from the single mutants.

Shifts in isotopic spectral centroids were used to determine levels of deuterium incorporation. Flexible and accessible peptides, such as would be predicted at the N-terminal extension, should have undergone a more rapid incorporation of deuterium than peptides that were more buried. For example, the mass of the N-terminal peptic peptide, residues 1–18, shifted to a higher mass at 15 sec, with no further shift with time (Fig. 2a). In contrast, in the interface peptic peptide, residues 53–70, the shift in mass peaks was slower (Fig. 2b), suggestive of a less accessible region, such as would be expected at the buried interface.

3.3. Differential local HDMS for each domain of WT βB2

Hydrogen exchange levels of peptic fragments were compared between different regions of WT βB2. Representative peptic fragments are shown in Figs. 3–4. The relative deuterium levels ranged from 0.5 Da to 6.0 Da. These levels are comparable to levels in similar size fragments where there is protection from exchange (Engen 2009;Wales et al., 2008). Wildtype βB2 was analyzed in three sets of experiments (Figs 3–5) utilizing two different mass spectrometers. There was an overall low level of incorporation in βB2-crystallin and the initial incorporation in the C-td peptides was lower than in the N-td peptides. These results were the same in all experiments, although the absolute values varied due to differences in chromatography and instrumentation.

Data from a representative experiment is listed in Table 1. Solvent accessibility was derived from the total number of incorporated deuterium as the percent of the total theoretically exchangeable amide hydrogen in that peptide (Yan, et al., 2002 and 2004). Incorporation in peptides in the N-td, amino acids 22–93, was 7–26% and in the C-td, amino acids 111–186, was 4 to 11%. This low level of incorporation in peptides ranging from 10–22 amino acids long is consistent with a low level of total incorporation from the global analyses. The deuterium content of the C-td peptides continued to increase with time reaching levels observed in the corresponding N-td peptides. The N- and C-td had similar numbers of exchangeable hydrogen, but different rates of incorporation.

Not all of the amide backbone hydrogen exchanged. Therefore, the relative deuterium was also calculated as the percent of total hydrogen that exchanged by 24 h (Eq. 2 in methods). This also allowed comparison of different experiments and to correct for possible differences in back exchange. Two independent experiments were compared. In the N-td

between residues 22–93, the average percent deuterium in 6 overlapping peptides was 64±13% at 15 sec (Fig. 3). In the C-td between residues 111–186, the average percent deuterium of 8 overlapping peptides was 37±11% with similar size peptides. Similar data were obtained in a separate experiment, in which average percent incorporation was 74±12% for residues 22–93 and 44±15% for residues 111–175 (Fig. 4 and Table 1, 24 h data not shown). The N-td had higher levels of incorporation than peptides in the C-td at the early time points, reflecting the greater solvent accessibility of the N-td.

Peptic peptide 53–71 in the N-td corresponds to peptide 143–164 in the C-td. These peptides contain the interface Gln70 and Gln162. The initial deuterium level in this N-td peptide was twice that in the corresponding C-td peptide suggesting greater solvent accessibility surrounding Gln70 (Fig. 3). The low level of deuterium incorporation, 0.5–1.2 Da, in peptide 151–164 further supported that this peptide at the predicted interface was buried (Fig. 3 and Table 1).

In peptic peptide 94–110, containing the linker between the domains, deuterium levels either did not increase or increased very little with time (Fig. 3D and 4E). Of the hydrogen that exchanged, almost all were exchanged immediately. However, the total deuterium incorporation of around 2 Da represented 9–13% of the total backbone amide hydrogen and suggested a generally low accessibility in solution, but comparable to other peptides in the N-td. The exchangeable hydrogen in this peptide may be exchanging in the linker only, residues 99–106, with the other amino acids buried in the domains. No other overlapping peptides containing the connecting peptide were obtained. This suggested that these regions were resistant to proteolysis, which is consistent with a compact structure of βB2, including these regions. Likewise initial deuterium levels in peptide 1–21 were the same at the later time points (Fig 3). This peptide contains the N-terminal extension at residues 1–16, in which the rapid initial incorporation of deuterium may occur as seen in Fig. 2a for peptide 1–18.

3.4. Deamidation-induced local structural perturbation of βB2

The hydrogen/deuterium exchange levels were compared between WT and the single mutants, Q70E and Q162E, and data for each peptide from 15 sec to 24 h are shown in Fig. 3a-h. Samples were handled identically and masses were measured on the same day to minimize any potential differences in chromatography that might affect back exchange (see methods). In the βB2-crystallin crystal structure the interface Gln are oriented towards the opposite domain of their partner subunit.

Deamidation mimicked at either of the interface Gln tended to decrease deuterium exchange-in at peptides in the N-td, including the interface peptide (Fig. 3a-c). Neither mutation altered the hydrogen exchange-in in the linker peptide between the domains (Fig. 3d) or in peptide 117–131 (Fig. 3f). Differences were most noted in the less accessible C-td. Deamidation mimicked at Q70 in the N-td increased deuterium levels in the interface peptide 143–164 and to a lesser degree in the peptide 151–164 (Fig. 3g and h). However, deamidation mimicked at Q162 did not icrease, but decreased deuterium levels in the homologous interface in the N-td (Fig. 3b) and at peptide 111–126, an outside loop region (Fig. 3e).

Therefore, deamidation at Q70 in the N-td increased solvent accessibility in the C-td interface peptide, while deamidation at the homologous Gln, Q162, decreased solvent accessibility at the homologous N-td interface peptide. This suggested differences between these sites that were not readily apparent from the crystal structure (Michiel et al., 2010).

The hydrogen/deuterium exchange levels were also compared between WT and DM. The relative deuterium level of WT, the N-td in particular, in Fig. 4 was about 30% less than in the separate experiment shown in Fig. 3. It was noted that the peptides in Fig. 4 eluted about a minute later during chromatography than those in Fig. 3 and may have potentially had more back exchange. Thus, relative deuterium levels were compared between WT and DM analyzed at the same time and reported in Fig. 4 for each peptic peptide from 15 sec to 60 min in Fig 4a-i. For the DM, only a few peptides were recovered at 24 h, which may be due to the greater tendency of DM to unfold and precipitate. Similar to the single mutants, there was decreased incorporation in peptide 71–93 (Fig. 4d). Similar to Q70E, there was increased incorporation in the C-td peptides, 132–186 (Fig. 4g-i). Additionally, there were small increases in deuterium incorporation in peptides 1–21 and 53–70 (Fig. 4a and c) and no change in peptides 22–52 and 94–131 (Fig. 4b, e-f). Separate samples were prepared and analyses repeated at four min with standard error reported. The error was less than 10% as was expected for similar HDMS experiments (Iacob, et al., 2009;Yan, et al., 2004) with only peptide 71–93 with error over ±0.2 Da.

Introducing deamidation at both interface Gln led to decreased solvent accessibility on an outside loop similar to both Q70E and Q162E; to increased solvent accessibility at the C-td interface peptide similar to Q70E; and to a small increase in exposure at the N-td interface peptide, where a small decreased had been observed for the single mutants. The greater increase in accessibility of the DM and Q70E compared to Q162E provide a structural basis for the increased tendency of these mutants to aggregate during thermal denaturation (Michiels et al., 2010).

3.5. Summary of deamidation-induced changes in solvent accessibility and evaluation of back exchange

Hydrogen/deuterium exchange levels were measured on a high-resolution mass spectrometer and three independent sets of samples were prepared for WT and two for DM. The relative deuterium levels in Fig. 5 varied only about 10–30% from those in Figs. 3 and 4 even with differences in desalting time and in chromatography between the different methods that would have contributed to differences in back exchange. Within experiments, samples were handled the same and differences between WT and mutant peptides reflected differences in deuterium incorporation during the exchange-in period.

Representative peptides 71–84, 94–110, 111–126, and 151–164 are shown in Fig. 5a-d. There was decreased deuterium incorporation in the DM peptide 72–93 at the later time points and increased incorporation in peptide 151–164 as reported in Fig. 4. There was also a small decrease in deuterium incorporation in peptide 94–110 and increase in peptide 111–126 in the DM that was not observed in Fig. 4. However, these differences were consistent with the overall trends reported in Fig. 4 of decreased deuterium incorporation in the N-td in the peptide adjacent to the site of deamidation and increased deuterium in the C-td.

Figure 6 summarizes the differences in hydrogen/deuterium exchange between each mutant and WT. Differences in relative deuterium levels were overlaid onto the reported 3D structure (PDB: 1YTQ, Smith et al., 2007). Differences from WT were separated into subtle, moderate, and substantial increases/decreases similar to previously described (Iacob et al., 2009). Figure 6a depicts the substantial increase in accessibility of Q70E at the C-td interface peptide (peptide highlighted in red). A decrease or no change in accessibility was observed in the N-td. In contrast, the Q162E mutant (Fig. 6b) had decreased accessibility in both domains (peptides highlighted in blue and green). In observing the affects of both mutations together, the DM (Fig. 6c) experienced a subtle increase in accessibility at both interface peptides (peptides highlighted in yellow) and additional changes further into the domains. Peptides 72–93 and 151–164 are highlighted in Fig. 6d. The contact areas

surrounding these peptides are also highlighted and the solvent accessibility is overlaid onto the ribbon structure (Viewer Pro Software, Accelrys, Inc., San Diego, CA, Solvent surface using a probe radius of 1.4)

4. Discussion

In cataractous and aged lenses extensively deamidated crystallins were found in the insoluble proteins (Wilmarth et al., 2006). Numerous studies by our laboratory and others have demonstrated that deamidation decreases crystallin stability (Flaugh et al., 2006; Gupta et al., 2006; Harms et al., 2004; Lampi et al., 2006; Takata et al., 2007). We have recently reported that deamidation at Q70 and Q162 decreased stability when perturbed during heating and increased the unfolding, aggregation, and precipitation of βB2 (Michiel et al., 2010). This decreased stability is due to the structural changes induced by deamidation that were detected in this study by hydrogen/deuterium exchange of the backbone amide hydrogen.

4.1. In-solution dynamics of βB2-crystallin

In the WT βB2-crystallin the low exchange of backbone amide hydrogen of about 20% suggests an overall low solvent accessibility of βB2-crystallin in solution. This is consistent with a tightly packed domain structure observed in the crystal structure. This compact structure of βB2, even at concentrations well below those found in the lens, contributes to its longevity and stability, which is needed for lens transparency.

Differences in initial levels of deuterium incorporation between the N- and C-terminal domains suggested a more highly accessible N-td and a more compact C-td. Despite the high homology between the two domains in the crystal structure, the more accessible N-td suggested there were differences in solution. The more compact C-td would be predicted to be more stable, as has been previously reported. During in vitro denaturation of βB2 the dimer unfolds by dissociating into monomers with a partially unfolded N-td and folded C-td (Evans et al., 2008; Fu and Liang, 2002; Wieligmann et al., 1999). The more exposed and flexible N-td unfolds more readily than the more compact C-td.

Hydrogen/deuterium exchange in peptides containing the N-terminal extension and the connecting peptide were expected to have more deuterium incorporation than the domains themselves, based on the exposure of these regions in the crystal structure. However, deuterium incorporation in these regions was similar to other regions in the protein. Several possible reasons are a greater percentage of residues buried in the domains than were exposed (for example, only half of the residues in peptide 94–110 are in the linker) or a high intrinsic rate of exchange that correlates to rapid back-exchange (Wales et al., 2008). However, the linker residues, 99–106, or the extension 1–16 were not calculated to have a high intrinsic rate of exchange (HXPep software and personal communication, Dr. John Engen, Northeastern University), and therefore, back exchange is not expected to be greater than in other peptides. However, additional interactions in solution not readily apparent in the crystal structure could have also led to their decreased accessibility.

4.2. Alteration of the local structure of βB2 due to deamidation

Mimicking deamidation by introducing charges at the domain-domain interface in βB2 both increased and decreased accessibility in the domains. Differences in accessibility suggested that deamidation at the N-td interface Gln disrupted the more compact C-td, while deamidation at the C-td interface Gln induced interactions within the more exposed N-td. Deamidation at Q70 disrupted the structure to a greater extent than deamidation at Q162 (Fig. 6). Disruption of the more compact C-td provides an explanation for the greater affect

on solubility and aggregation of deamidation at Gln70 in comparison to Gln162, despite the homologous contacts surrounding the two Gln (Michiel et al., 2010).

Introducing deamidation-induced charge repulsion at the interface in βB2 by mutating both interface Gln increased accessibility at both N- and C-td interface residues and affected peptides beyond the interface. Of note is the decrease in accessibility of an outside loop in the N-td (Fig. 6D). The increased accessibility suggested a loosening of interactions at the interface, with perhaps a compensatory decrease in an outside loop region. These structural changes are supported by our previous observations of tertiary changes in the structure of the DM, which are not observed in the single mutants (Lampi et al., 2006).

The domain interface in βB2 is stabilized by hydrophobic interactions and hydrogen bonding (Lappato et al., 1991). The energy differences during unfolding of deamidated βB2 corresponded to one or two hydrogen bonds being disrupted (Lampi et al., 2006). Therefore, the increased accessibility and hydrophobicity observed in this study may result from the disruption of only one or two hydrogen bonds. In contrast, decreases in accessibility may be due to deamidation inducing new interactions. For example, the N-terminal extension in the single mutants may interact with the newly introduced charge in the interface and cover previously exposed regions in the N-td. We have previously reported a similar decrease in the flexibility of the N-terminal extension when deamidation was mimicked at the interface Gln in the C-td of βB1 (Lampi et al., 2002).

The decreased accessibility of the N-td may prevent interaction of deamidated βB2 with α-crystallin chaperone. During unfolding it is the intermediate with an unfolded N-td that has been proposed to interact with the protective chaperone, α-crystallin (Evans et al., 2008). Therefore, the decreased accessibility in the N-td may have prevented α-crystallin from completely rescuing deamidated βB2 from precipitation (Michiel et al., 2010). The greater aggregation of Q70E or DM due to the greater structural perturbations identified in this study could also have prevented α-crystallin from interacting with βB2.

We have identified local conformational changes due to deamidation that increased the propensity of βB2-crystallin to aggregate (Michiel et al., 2010). Even these small changes in structure can significantly alter solubility and function of the crystallins, as has recently been reported for the cataract causing P23T mutation in γD-crystallin (Jung et al., 2009). Deamidation at the interacting interface both increased and decreased exposure, with disruption of the more compact C-td having a greater effect on stability. In the highly concentrated milieu within the lens fiber cells, deamidation may disrupt the interfaces within and between crystallin subunits. An accumulation of deamidation-induced changes in local structural dynamics may contribute to protein insolubility and the inability of α-crystallin to completely rescue a partially unfolded intermediate, contributing to cataract formation.

Acknowledgments

The authors wish to thank Drs. Max Deinzer and Claudia Maier for their considerable help and guidance and Jason Lampi and Leonel Trujillo for their expert technical help. We are also very grateful to Portland State University for the use of the LTQ-Orbitrap Discovery (National Science Foundation, Grant# 0741993), to Oregon State University's Mass Spectrometry core facility, and to NIH for grants EY012239 (K.J.L.) and core grant EY10572 (L.L.D.), and to Dr. Tatsuo Tomita for addition financial support.

Abbreviations

MW	molecular weight
SDS-PAGE	sodium dodecyl sulfate - polyacrylamyde gel electrophoresis

3D	three dimensional
bis-ANS	4,4′-Bis (1-anilinonaphthalene 8-sulfonate)
MES	2-(4-Morpholino)-Ethane Sulfonic Acid

References

Bax B, Lapatto R, Nalini V, Driessen H, Lindley PF, Mahadevan D, Blundell TL, Slingsby C. X-ray analysis of betaB2-crystallin and evolution of oligomeric lens proteins. Nature 1990;347:776–80. [PubMed: 2234050]

Delaye M, Tardieu A. Short-range order of crystallin proteins accounts for eye lens transparency. Nature 1983;302:415–7. [PubMed: 6835373]

Engen JR. Analysis of protein conformation and dynamics by hydrogen/deuterium exchange MS. Anal Chem 2009;81:7870–5. [PubMed: 19788312]

Englander SW, Sosnick TR, Englander JJ, Mayne L. Mechanisms and uses of hydrogen exchange. Curr Opin Struct Biol 1996;6:18–23. Review. [PubMed: 8696968]

Evans P, Slingsby C, Wallace BA. Association of partially folded lens betaB2-crystallins with the alpha-crystallin molecular chaperone. Biochem J 2008;409:691–9. [PubMed: 17937660]

Flaugh SL, Mills IA, King J. Glutamine deamidation destabilizes human gammaD-crystallin and lowers the kinetic barrier to unfolding. J Biol Chem 2006;281:30782–93. [PubMed: 16891314]

Fu L, Liang JJ. Unfolding of human lens recombinant betaB2- and gammaC-crystallins. J Struct Biol 2002;139:191–8. [PubMed: 12457849]

Gupta R, Srivastava K, Srivastava OP. Truncation of motifs III and IV in human lens betaA3-crystallin destabilizes the structure. Biochemisry 2006;45:9964–78.

Hains PG, Truscott RJ. Post-translational modifications in the nuclear region of young, aged, and cataract human lenses. J Proteome Res 2007;6:3935–43. [PubMed: 17824632]

Hanson SR, Hasan A, Smith DL, Smith JB. The major in vivo modifications of the human water-insoluble lens crystallins are disulfide bonds, deamidation, methionine oxidation and backbone cleavage. Exp Eye Res 2000;71:195–207. [PubMed: 10930324]

Harding JJ. Nature and origin of the insoluble protein of rat lens. Exp Eye Res 1969;8:147–56. [PubMed: 5786864]

Harms MJ, Wilmarth PA, Kapfer DM, Steel EA, David LL, Bächinger HP, Lampi KJ. Laser light-scattering evidence for an altered association of betaB1-crystallin deamidated in the connecting peptide. Protein Sci 2004;13:678–86. [PubMed: 14978307]

Houde D, Arndt J, Domeier W, berkowitz S, Engen JR. Characterization of IgG1 conformation and conformational dynamics by hydrogen/deuterium exchange mass spectrometry. Anal Chem 2009;81:2644–51. [PubMed: 19265386]

Iacob RE, Pene-Dumitrescu T, Zhang J, Gray NS, Smithgall TE, Engen JR. Conformational disturbance in Abl kinase upon mutation and deregulation. Proc Natl Acad Sci USA 2009;106:1386–91. [PubMed: 19164531]

Jung J, Byeon IJ, Wang Y, King J, Gronenborn AM. The structure of the cataract causing P23T mutant of Human gammaD crystallin exhibits local distinctive conformational and dynamic changes. Biochemistry 2009;48:2597–609. [PubMed: 19216553]

Lampi KJ, Amyx KK, Ahmann P, Steel EA. Deamidation in human lens betaB2-crystallin destabilizes the dimer. Biochemistry 2006;45:3146–53. [PubMed: 16519509]

Lampi KJ, Oxford JT, Bächinger HP, Shearer TR, David LL, Kapfer DM. Deamidation of human betaB1 alters the elongated structure of the dimer. Exp Eye Res 2001;72:279–88. [PubMed: 11180977]

Lapatto R, Nalini V, Bax B, Driessen H, Lindley PF, Blundell TL, Slingsby C. High resolution structure of an oligomeric eye lens beta-crystallin. Loops, arches, linkers and interfaces in beta B2 dimer compared to a monomeric gamma-crystallin. J Mol Biol 1991;222:1067–83. [PubMed: 1762146]

Liu BF, Liang JJ. Domain interaction sites of human lens betaB2-crystallin. J Biol Chem 2006;281:2624–30. [PubMed: 16319073]

Michiel M, Duprat E, Skouri-Panet F, Lampi JA, Tardieu A, Lampi KJ, Finet S. Aggregation of deamidated human betaB2-crystallin and incomplete rescue by alpha-crystallin chaperone. Exp Eye Res. 2010 in press.

Nalini V, Bax B, Driessen H, Moss DS, Lindley PF, Slingsby C. Close packing of an oligomeric eye lens beta-crystallin induces loss of symmetry and ordering of sequence extensions. J Mol Biol 1994;236:1250–8. [PubMed: 8120900]

Perkins DN, Pappin DJ, Creasy DM, Cottrell JS. Probability-based protein identification by searching sequence databases using mass spectrometry data. Electrophoresis 1999;20:3551–67. [PubMed: 10612281]

Resnikoff S, Pascolini D, Etya'ale D, Kocur I, Pararajasegaram R, Pokharel GP, Mariotti SP. Global data on visual impairment in the year 2002. Bull World Health Organ 2004;82:844–51. [PubMed: 15640920]

Searle BC, Dasari S, Wilmarth PA, Turner M, Reddy AP, David LL, Nagalla SR. Identification of protein modifications using MS/MS de novo sequencing and the OpenSea alignment algorithm. J Proteome Res 2005;4:546–54. [PubMed: 15822933]

Smith MA, Bateman OA, Jaenicke R, Slingsby C. Mutation of interfaces in domain-swapped human betaB2-crystallin. Protein Sci 2007;16:615–25. [PubMed: 17327390]

Takata T, Oxford JT, Brandon TR, Lampi KJ. Deamidation alters the structure and decreases the stability of human lens betaA3-crystallin. Biochemistry 2007;46:8861–71. [PubMed: 17616172]

Takata T, Woodbury LG, Lampi KJ. Deamidation alters interactions of beta-crystallins in hetero-oligomers. Mol Vis 2009;15:241–9. [PubMed: 19190732]

Truscott RJ, Augusteyn RC. Changes in human lens proteins during nuclear cataract formation. Exp Eye Res 1977;24:159–70. [PubMed: 844510]

Van Montfort RL, Bateman OA, Lubsen NH, Slingsby C. Crystal structure of truncated human betaB1-crystallin. Protein Sci 2003;12:2606–12. [PubMed: 14573871]

Wales TE, Fadgen KE, Gerhardt GC, Engen JR. High-speed and high-resolution UPLC separation at zero degrees Celsius. Anal Chem 2008;80:6815–20. [PubMed: 18672890]

Weis DD, Engen JR, Kass IJ. Semi-automated analysis of hydrogen exchange mass spectra using HX-Express. J Am Soc Mass Spectrom 2006;17:1700–3. [PubMed: 16931036]

Wieligmann K, Mayr EM, Jaenicke R. Folding and self-assembly of the domains of betaB2-crystallin from rat eye lens. J Mol Biol 1999;286:989–94. [PubMed: 10047476]

Wilmarth PA, Tanner S, Dasari S, Nagalla SR, Riviere MA, Bafna V, Pevzner PA, David LL. Age-related changes in human crystallins determined from comparative analysis of post-translational modifications in young and aged lens: does deamidation contribute to crystallin insolubility? J Proteome Res 2006;5:2554–66. [PubMed: 17022627]

Yan X, Zhang H, Watson J, Schimerlik MI, Deinzer ML. Hydrogen/deuterium exchange and mass spectrometric analysis of a protein containing multiple disulfide bonds: Solution structure of recombinant macrophage colony stimulating factor-beta (rhM-CSFbeta). Protein Sci 2002;11:2113–2124. [PubMed: 12192067]

Yan X, Broderick D, Leid M, Schimerlik MI, Deinzer ML. Dynamics and Ligand-Induced Solvent Accessibility Changes in Human Retinoid X Receptor Homodimer Determined by Hydrogen Deuterium Exchange and Mass Spectrometry. Biochemistry 43 2004;4:909–917.

Yan X, Maier C. Hydrogen/Deuterium Exchange Mass Spectrometry. Mass Spectrometry of Proteins and Peptides 2009;494:255–271.

Zhang Z, Smith DL. Determination of amide hydrogen exchange by mass spectrometry: a new tool for protein structure elucidation. Protein Sci 1993;2:522–31. [PubMed: 8390883]

Zhang Z, Smith DL, Smith JB. Human beta-crystallins modified by backbone cleavage, deamidation and oxidation are prone to associate. Exp Eye Res 2003;77:259–72. [PubMed: 12907158]

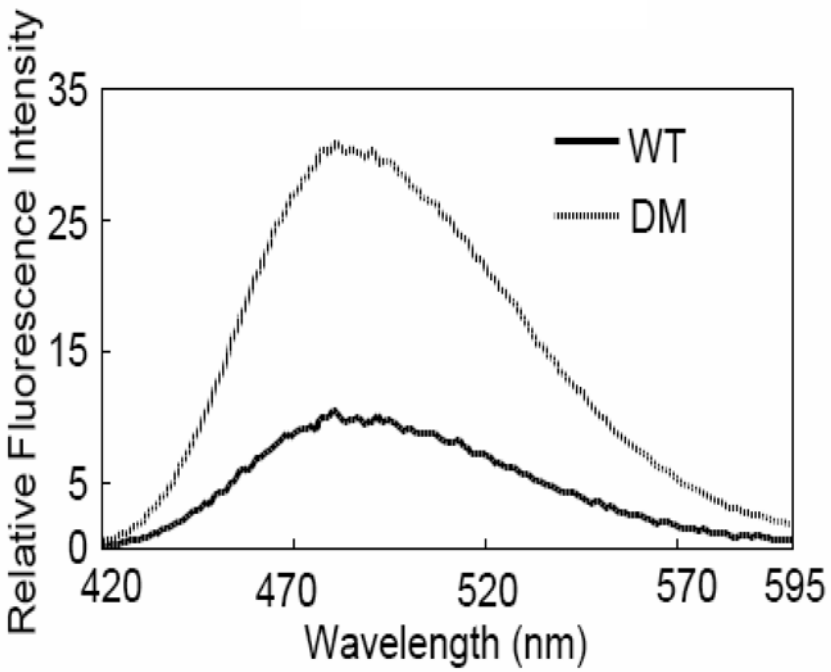

Fig. 1. bis-ANS fluorescence for WT and Q70E/Q162E (DM) βB2-crystallin

Emission spectra of WT and DM as measured by fluorescence spectrometry at 395 nm. WT is showed as a bold line and DM as a dotted line. Intensity was greater for DM, suggesting buried hydrophobic surfaces were exposed in DM compared to WT.

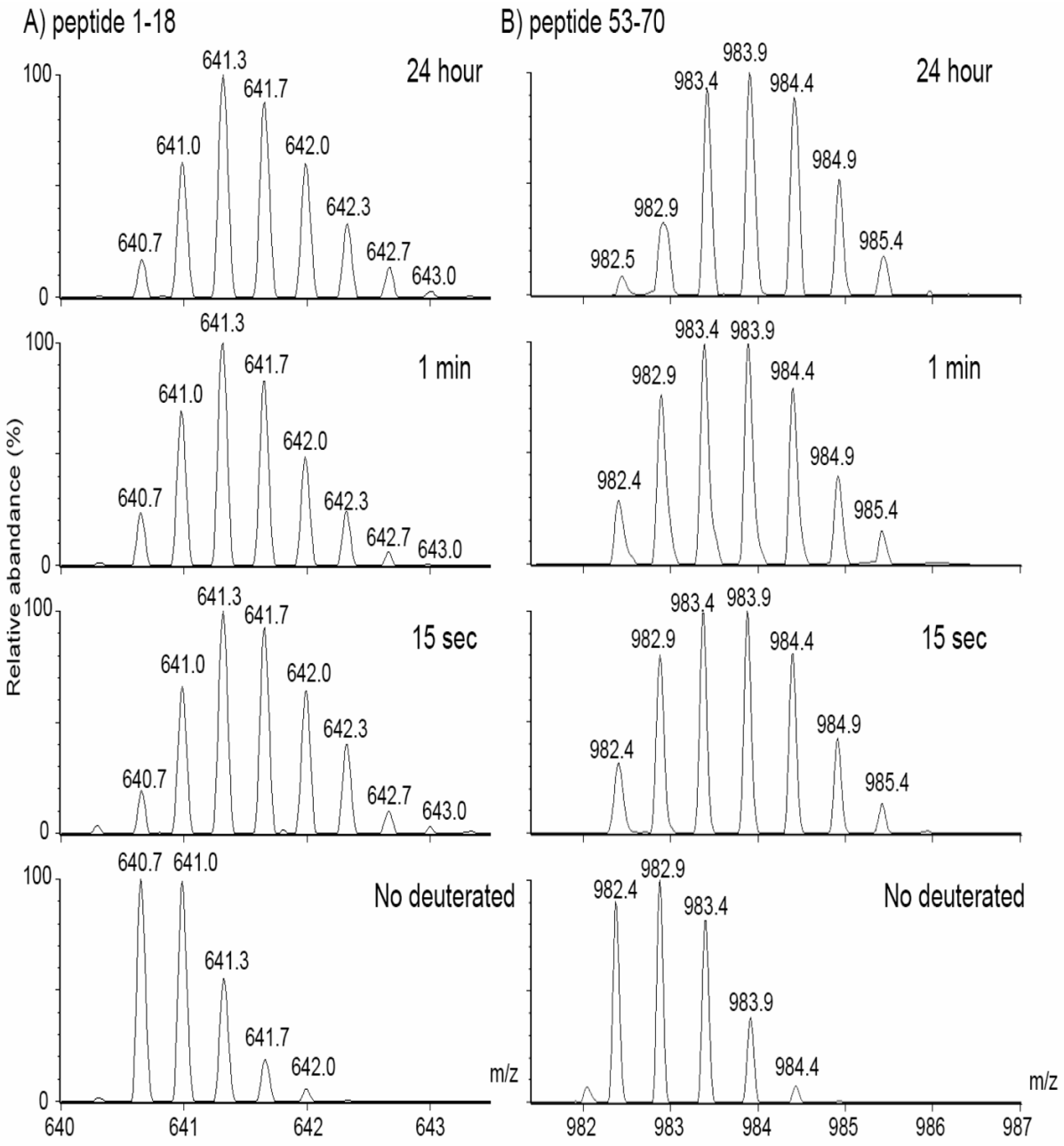

Fig. 2. Isotopic peak distributions of deuterated peptide masses (m/z) from WT β B2

WT was incubated in D_2O buffers for 0, 15 sec, 1 min, and 24 h and then digested with pepsin. A) The triply charged form of the N-terminal peptide, residues 1–18, shows a shift to higher mass at 15 sec with deuterium incorporation. No further increase in mass was detected with time. B) The doubly charged form of the interface peptide, residues 53–70, shows a more gradual shift in peak heights to a higher mass and therefore, a slower incorporation of deuterium.

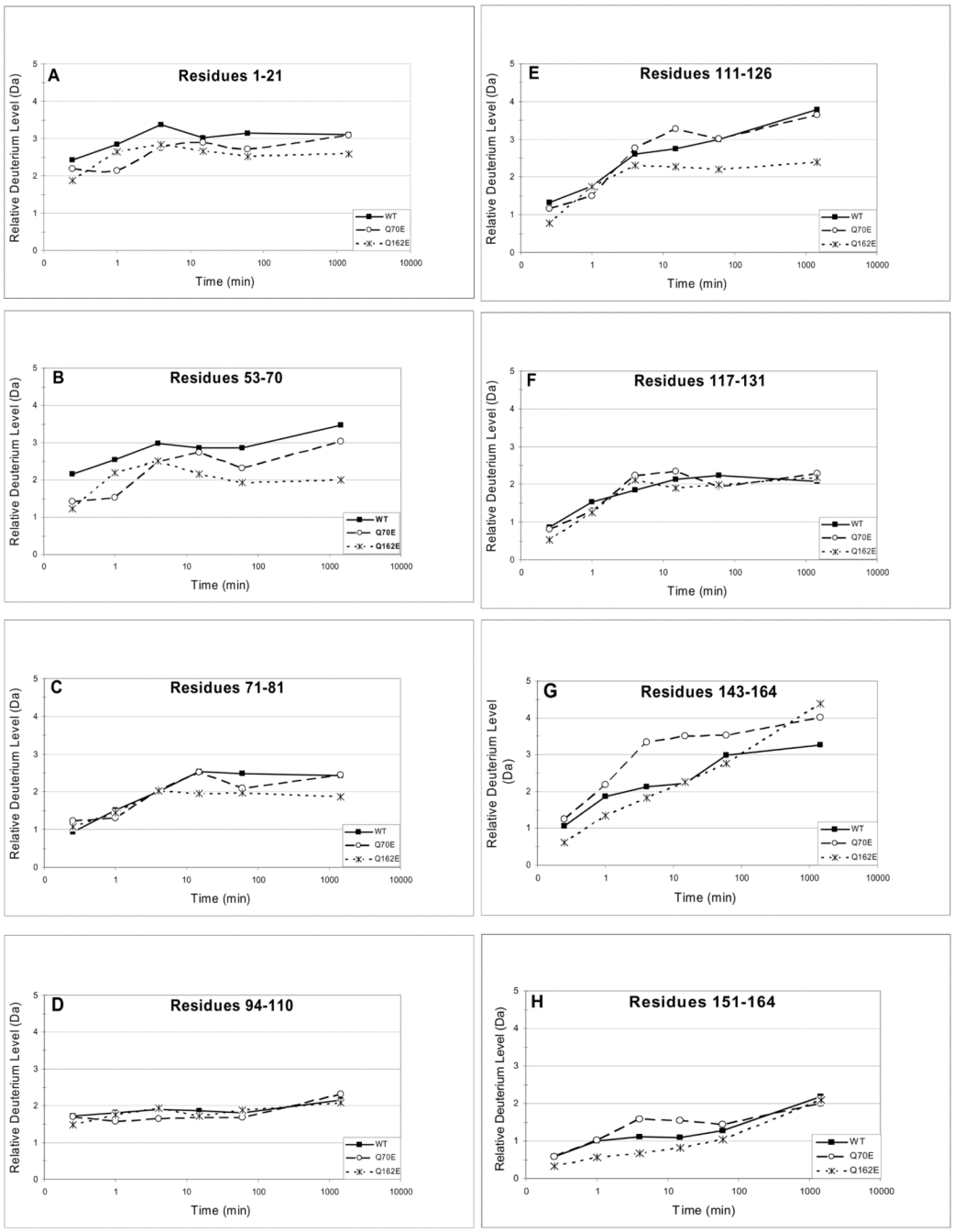

Fig. 3. Hydrogen/deuterium exchange in Q70E and Q162E compared to WT βB2-crystallin

The relative deuterium incorporation (Da) (Eq. 1, Methods) at 15 sec, 1 min, 4 min, 15 min, 60 min and 24 h are shown for peptic peptides from WT, Q70E, and Q162E. The 8 representative peptides contain residues A) 1–21, B) 53–70, C) 71–81, D) 94–110, E) 111–126, F) 117–131, G) 143–164, and H) 151–164.

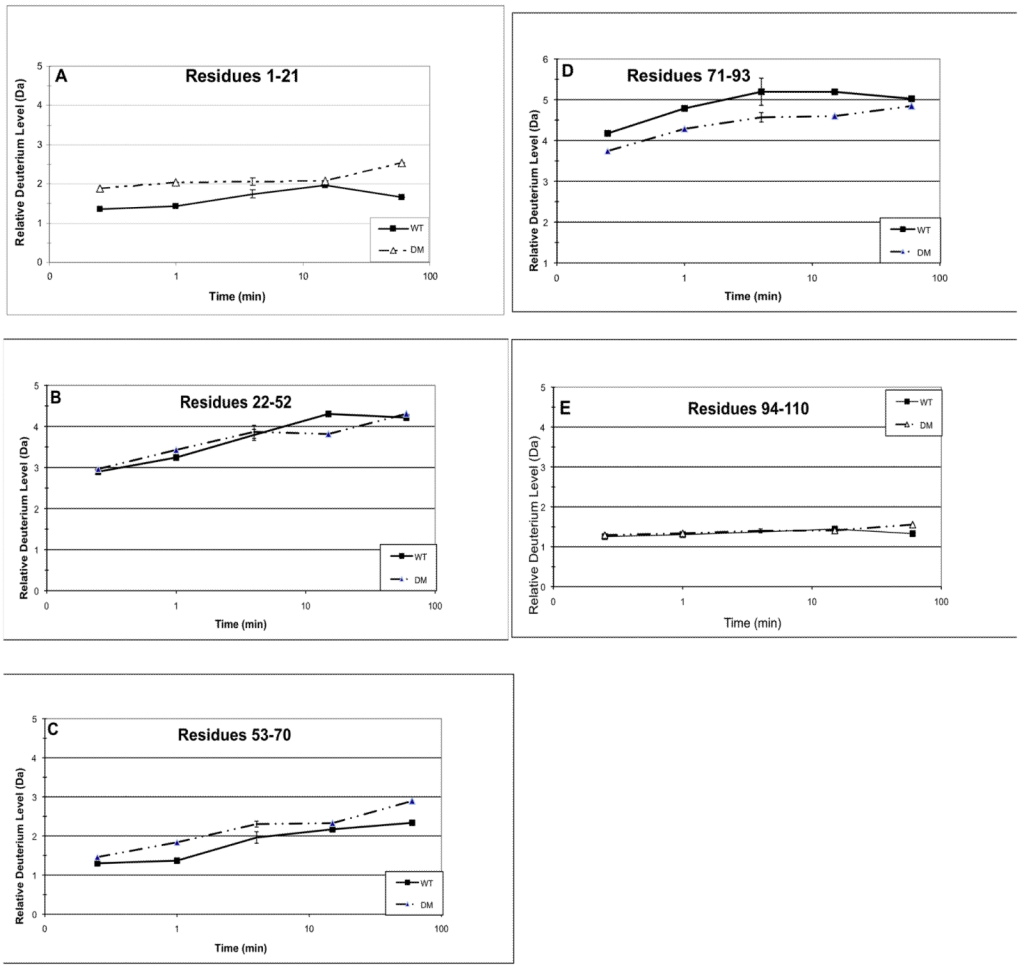

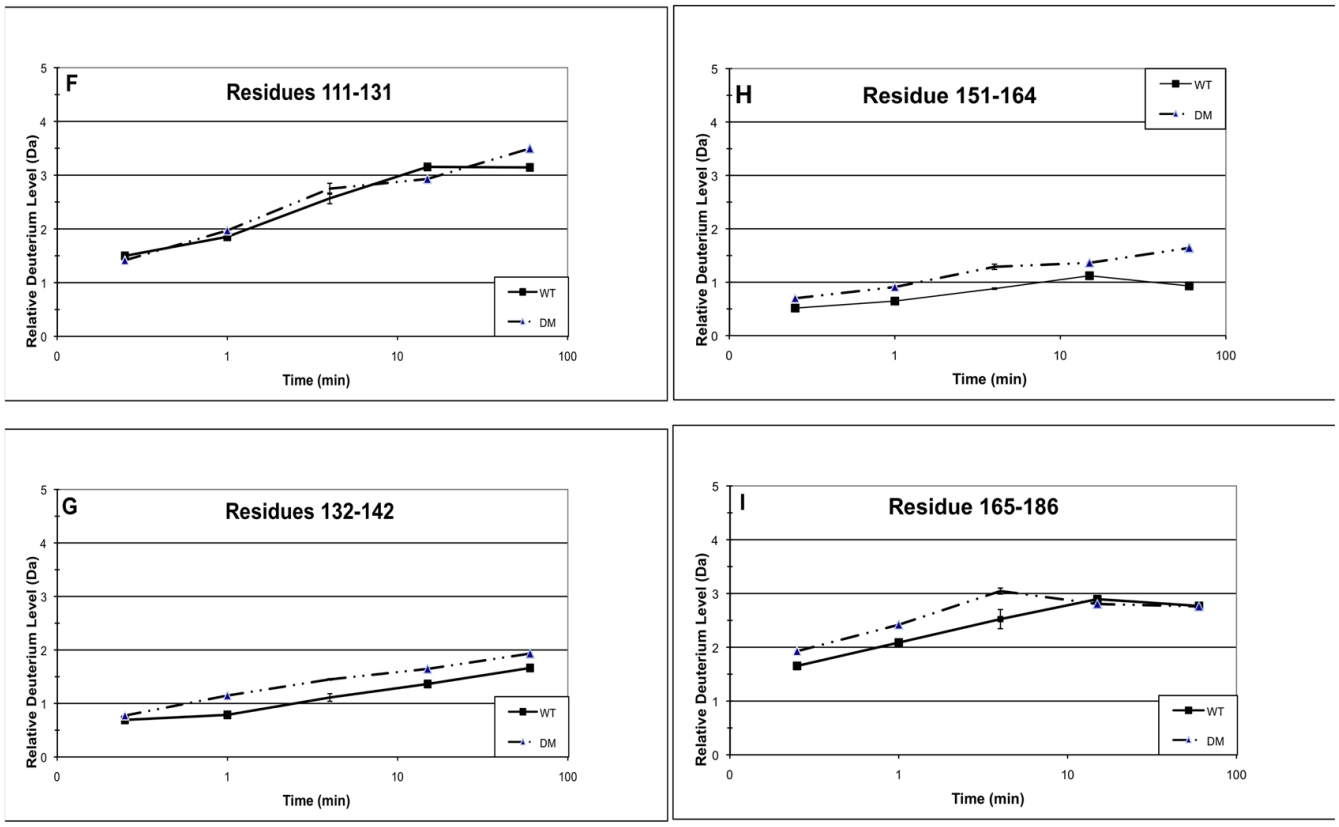

Fig. 4. Hydrogen/deuterium exchange in the double mutant Q70E/Q162E (DM) compared to WT βB2-crystallin

The relative deuterium levels (Da) (Eq. 1, Methods) at 15 sec, 1 min, 4 min, 15 min, and 60 min are shown for peptic peptides from WT and DM. The 9 representative peptides are residues A) 1–21, B) 22–52, C) 53–70, D) 71–93, E) 94–110, F) 111–131, G) 132–142, H) 151–164, and I) 165–186. Error bars are shown at 4 min for 2–3 independent experiments.

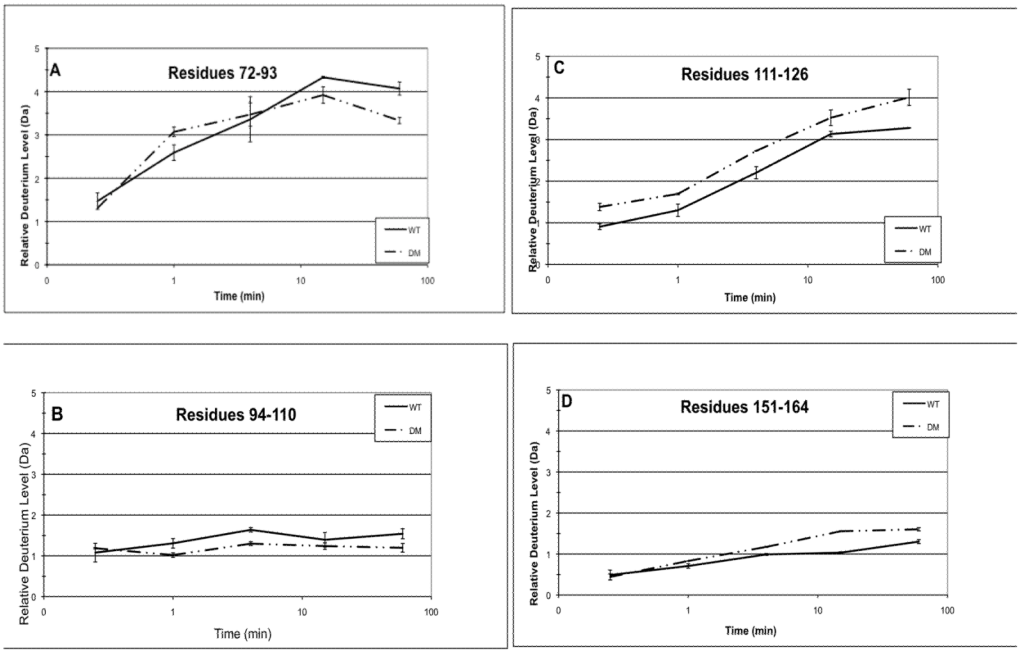

Fig. 5. Confirmation of differences in accessibility between WT βB2 and DM

Because HDMS is sensitive to back exchange, differences between WT and DM were confirmed in a separate set of experiments (see methods). The relative deuterium levels (Da) at 15 sec, 1 min, 4 min, 15 min, and 60 min are shown for peptic peptides from WT and DM. The 4 representative peptides are residues A) 72–93, B) 94–110, C) 111–126, and D) 151–164. Error bars are from 2–3 independent experiments.

Figure 6A and B

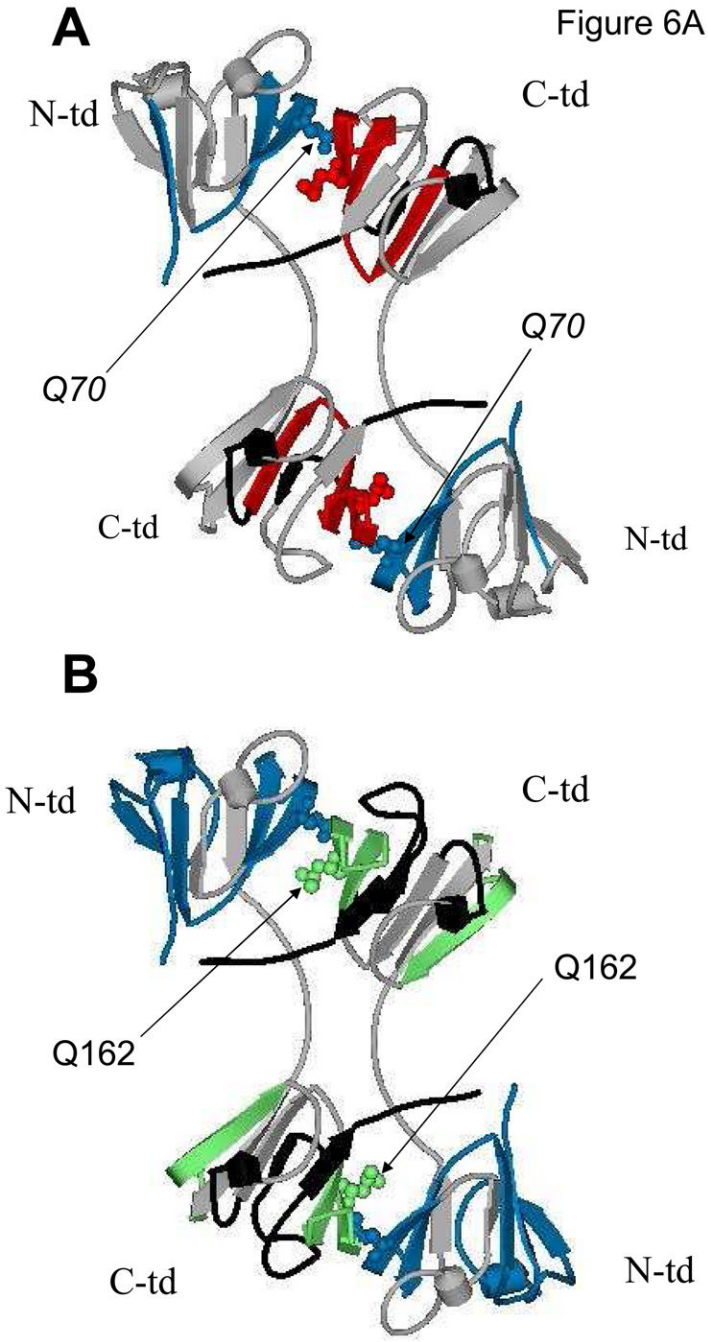

Figure 6C

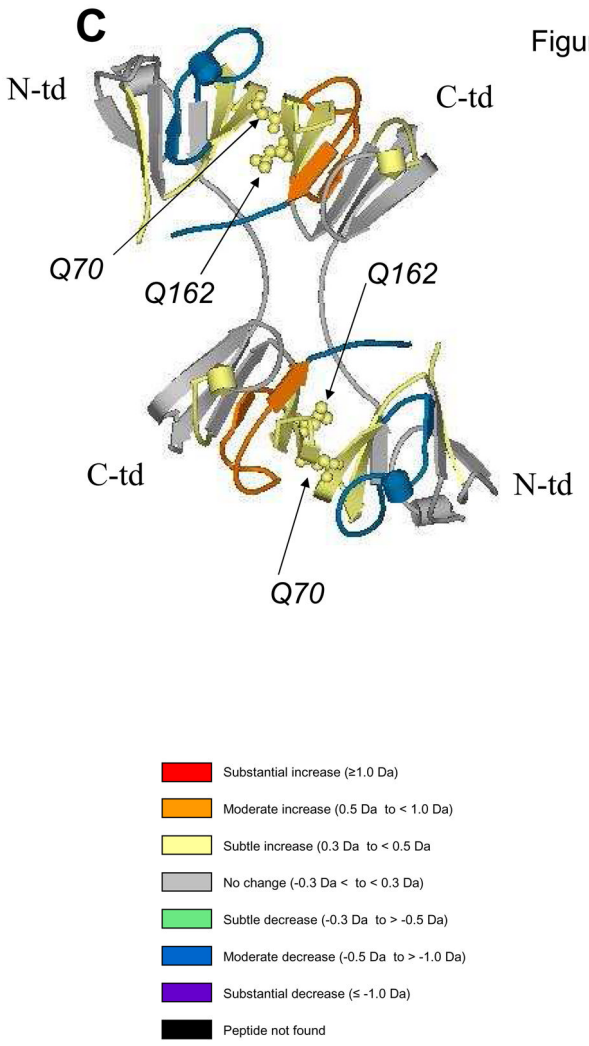

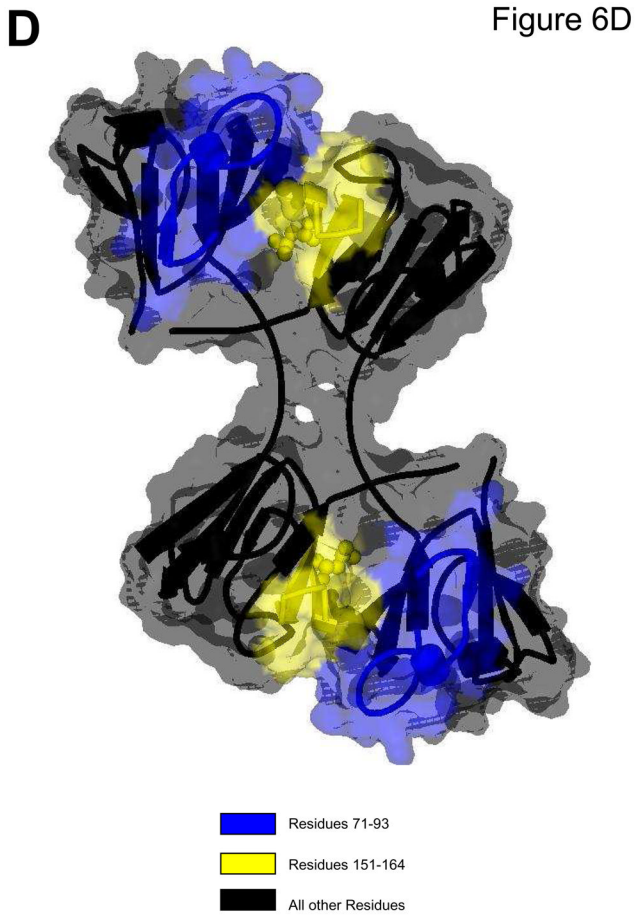

Fig. 6. Summary of conformation changes due to deamidation

The difference in relative deuterium levels between Q70E (A), Q162E (B), and DM (C) and WT βB2-crystallin were overlaid onto the human βB2-crystal structure (PDB:1YTQ). Data from 4 min were chosen to best represent differential trends between proteins, except in the case of residues 22–52 and 171–186 from Q70E, where data from 60 min was utilized. The color of the peptide indicates the differential trend between the mutant and the WT (Iacob, et al. 2009). Arrows indicate sites that were mutated to mimic deamidation. Interface glutamines 70 and 162 are shown in Cpk model representation on the structure. **(D)** A solvent space filling model of the βB2-crystallin dimer using a probe radius of 1.4 with the contact area surrounding residues 71–93 highlighted in blue and surrounding 151–164 in yellow. These peptides correspond to where the greatest changes were detected in Fig. 5.

Exp Eye Res. Author manuscript; available in PMC 2011 September 1.

Table 1

Solvent Accessibility in WT βB2 Fragments[a]

Peptide	0.25min	1min	4min	15min	60min
1–21[b]	7.2	7.5	9.2	10.3	8.7
22–52	10.0	11.2	13.1	14.8	14.5
53–70	7.7	8.1	11.5	12.8	13.7
71–81	10.7	11.7	15.4	18.8	17.2
82–93[c]	25.9	30.2	30.4	27.6	27.5
94–110[d]	9.3	9.7	10.2	10.3	9.8
111–116[c]	11.3	9.9	14.4	17.4	23.0
117–131	6.7	9.7	13.2	16.3	14.2
143–150	4.4	10.5	16.3	18.3	24.1
151–164	4.0	5.0	6.8	8.6	7.2
165–186	8.3	10.4	12.6	14.5	13.8

[a] Hydrogen exchanged as a percent of the total amide hydrogen in that peptide.

[b] Contains the N-td extension

[c] Peptides 82–93 and 111–116 were obtained by subtracting overlapping peptides.

[d] Contains the linker peptide